Original Article

Trends in Hearing
Volume 25: 1–19
© The Author(s) 2021
Article reuse guidelines:
sagepub.com/journals-permissions
DOI: 10.1177/23312165211061116
journals.sagepub.com/home/tia
SAGE

The Perception of Ramped Pulse Shapes in Cochlear Implant Users

Charlotte Amalie Navntoft[1,2], David M. Landsberger[3], Tania Rinaldi Barkat[2] and Jeremy Marozeau[1]

Abstract

The electric stimulation provided by current cochlear implants (CI) is not power efficient. One underlying problem is the poor efficiency by which information from electric pulses is transformed into auditory nerve responses. A novel stimulation paradigm using ramped pulse shapes has recently been proposed to remedy this inefficiency. The primary motivation is a better biophysical fit to spiral ganglion neurons with ramped pulses compared to the rectangular pulses used in most contemporary CIs. Here, we tested the hypotheses that ramped pulses provide more efficient stimulation compared to rectangular pulses and that a rising ramp is more efficient than a declining ramp. Rectangular, rising ramped and declining ramped pulse shapes were compared in terms of charge efficiency and discriminability, and threshold variability in seven CI listeners. The tasks included single-channel threshold detection, loudness-balancing, discrimination of pulse shapes, and threshold measurement across the electrode array. Results showed that reduced charge, but increased peak current amplitudes, was required at threshold and most comfortable levels with ramped pulses relative to rectangular pulses. Furthermore, only one subject could reliably discriminate between equally-loud ramped and rectangular pulses, suggesting variations in neural activation patterns between pulse shapes in that participant. No significant difference was found between rising and declining ramped pulses across all tests. In summary, the present findings show some benefits of charge efficiency with ramped pulses relative to rectangular pulses, that the direction of a ramped slope is of less importance, and that most participants could not perceive a difference between pulse shapes.

Keywords

cochlear implant, pulse shape, charge-saving, power consumption, psychophysics

Introduction

The electric stimulation delivered by current cochlear implants (CI) is not very power efficient. One underlying issue is the poor efficiency of how information in electric pulses is transmitted into neural responses. An inefficient electric pulse requires an increased level of charge to produce the same level of neural activity than an efficient one, ultimately consuming more stimulation power. The present study investigated whether a novel stimulation shape consisting of ramped pulses would reduce the amount of charge required to reach threshold and a given loudness level. If so, implementing these pulses into a sound coding strategy might reduce power consumption in CIs, which eventually may increase battery life or provide the opportunity to reduce the size of the battery.

Modern CI devices typically provide trains of brief symmetric, biphasic, charge-balanced pulses consisting of an anodic and cathodic rectangular phase of equal amplitude. However, this configuration is considered inefficient because the two phases of opposite polarity can partially cancel each other out (Guérit et al., 2018; Joshi et al., 2017a) when integrated by the neuronal membrane. This is demonstrated by the fact that the stimulation with a cathodic monophasic pulse leads to significantly lower thresholds than cathodic-first biphasic pulse in implanted cats (Miller et al.,

[1]Hearing Systems Group, Department of Health Technology, Technical University of Denmark, Kgs. Lyngby, Denmark
[2]Brain and Sound Lab, Department of Biomedicine, Basel University, Basel, Switzerland
[3]Department of Otolaryngology, New York University School of Medicine, New York, USA

Corresponding Author:
Jeremy Marozeau, Hearing Systems Group, Department of Health Technology, Technical University of Denmark, Ørsteds Plads, Building 352, Kgs. Lyngby 2800, Denmark.
Email: jemaroz@dtu.dk

1999) and that increasing interphase gap reduces thresholds and increases loudness in human CI listeners (Carlyon et al., 2005; Hardie & Shepherd, 1999; McKay & Henshall, 2003). However, monophasic pulses (either anodic or cathodic) are not safe to use in humans because the unbalanced electric stimulation can create oxidation products and damage both the ear and the electrodes (Brummer & Turner, 1977; Litovsky et al., 2017). A growing number of studies have therefore investigated if modified, charge-balanced versions of the biphasic, rectangular pulse shape could be more efficient. These alternative pulse shapes include biphasic pulses with a long interphase gap (Carlyon et al., 2005; McKay & Henshall, 2003), triphasic pulses (Bonnet et al., 2004), alternating monophasic pulses (Carlyon et al., 2005; Van Wieringen et al., 2005), pseudomonophasic pulses (Undurraga et al., 2012; Van Wieringen et al., 2005), alternating and/or delay pseudomonophasic pulses (Macherey et al., 2006). These shapes take advantage of polarity effects and/or of avoiding cancellation of the opposite phase(s) and have demonstrated lower thresholds and most comfortable levels (MCLs) compared to the commonly used biphasic pulses. Furthermore, recent evidence suggests that a novel ramped strategy for CI stimulation based on biophysics may provide a more efficient and controlled activation of spiral ganglion neurons (SGNs) (Ballestero et al., 2015; Navntoft et al., 2020; Yip et al., 2017).

The main argument for using a ramped pulse shape is that they are proposed to target ion channel dynamics in SGNs not engaged by rectangular pulses (Ballestero et al., 2015). SGNs, among other neurons in the auditory system, express depolarization-activated, outward, low-threshold potassium (KLT) channels (Mo et al., 2002; Smith et al., 2015). These channels make neurons sensitive to the rate at which they are depolarized. Studies in neurons from the cochlear nucleus and medial superior olivary have shown that the KLTs regulate neuronal firing by providing stronger phase locking (McGinley & Oertel, 2006; Rutherford et al., 2012; Smith et al., 2015) and lowering thresholds for the generation of action potentials (Ferragamo & Oertel, 2002; Svirskis et al., 2002). Using patch-clamp recordings in single-cultured SGNs, Ballestero et al. (2015) demonstrated that stimulus efficacy needed to evoke action potentials increased with a steeper stimulus slope. More specifically, activated KLT channels act as a high-pass filter that inhibits action potentials to slow depolarization. Only fast depolarization, which reaches threshold before a sufficient number of depolarization-activated KLT channels hyperpolarize the membrane potential, can trigger an action potential. This restricts the neuron to fire at the onset of a depolarization. The result is reduced jitter, improved phase locking, and rapid adaptation, as demonstrated in SGNs and medial superior olivary neurons using *in vitro* recordings (Johnston et al., 2010; Mo et al., 2002; Smith et al., 2015; Svirskis et al., 2002). The hyperpolarization mediated by activated KLT channels increases the threshold of a single neuron. However, the threshold of a compound potential is assumed to be reduced when all auditory nerve fibers in the proximity to the stimulating electrode are activated synchronously by a stimulus that depolarizes the membrane before KLT channels start acting. Thus, a fast depolarization of the membrane generated by a ramped electric pulse is thought to provide a more efficient SGN response via a delayed activation of KLTs. Indeed, including KLT channel dynamics in Hodgkin–Huxley type discrete cable models of the auditory nerve has improved predictions of the time course of refractoriness, adaptation, in particular to high stimulation rates, and accommodation (subthreshold adaptation) (Boulet et al., 2016; Bruce et al., 2019; Imennov & Rubinstein, 2009; Negm & Bruce, 2014; Schwarz et al., 1995). The same is true for model predictions of spike times and thresholds for monophasic pulses in simulated single auditory nerve fibers (Joshi et al., 2017b).

The large majority of *in vitro* studies cited above used a rising ramped current (Ballestero et al., 2015; Ferragamo & Oertel, 2002; McGinley & Oertel, 2006; Smith et al., 2015; Svirskis et al., 2002). This does not imply that neurons should be insensitive to a declining ramp. In fact, phasic neurons, including SGNs, are in general proposed to respond better to changing than to steady inputs (Gai et al., 2009; Izhikevich, 2007). A rising slope of the membrane potential would, however, be more beneficial than a declining one. This is mainly because the rising slope does not initially activate KLTs, as most of the current is delivered before the KLT conductance becomes too high to suppress firing, whereas the declining slope activates KLTs to begin with due to the onset needed to produce the declining ramp. This idea is supported by the work of Gai and colleagues. Using a stochastic sinusoidal input in a computational model and brainstem slice recordings, they demonstrated that a phasic neuron also responded to the declining part of the signal, although at a lower firing probability relative to the rising part (Gai et al., 2009, 2010). Furthermore, the sensitivity to both phases was largely dependent on the presence of KLT channels, again highlighting their role as "slope-detectors" (Gai et al., 2009). These findings are in line with our recent study, in which we characterized responses to biphasic ramped pulses using auditory brainstem recordings in CI-implanted mice (Navntoft et al., 2020). We found that less charge, but increased peak current amplitude, was needed to evoke responses with ramped shapes that were similar in amplitude to responses with rectangular shapes. Furthermore, a pulse shape with a rising ramp over both phases was more charge-efficient than a pulse shape with a declining ramp over both phases. Despite the different experimental setups used in those two studies (including intra- vs. extracellular stimulation, mono- vs. biphasic pulses, time scales, readout, etc.) (Gai et al., 2009; Navntoft et al., 2020), both suggest a higher sensitivity to the rising compared to the declining portion of an input signal and that

any ramp is more efficient in generating neural responses than rectangular pulses. The exact mechanism of how an extracellular biphasic CI pulse with a ramp affects the rate of membrane potential changes and consequently the engagement of ion channels, including KLT, dynamics is as yet unclear. Additional modeling or animal studies may be required to provide further insight into the mechanism.

To date, only one study has examined the potential of stimulation with a non-rectangular pulse shape in human CI users. Without taking KLT channels into account, Yip et al. (2017) coupled an auditory nerve model with a genetic algorithm to find the most energy-efficient pulse shape. A non-rectangular pulse shape with an exponentially decaying cathodic phase and an approximated rectangular anodic phase turned out to produce energy savings of 20%–30% compared to a rectangular shape. The authors hereafter did a simple loudness task with biphasic exponential waveform (decaying exponential cathodic, growing exponential anodic) in four human CI users and found a 26% charge reduction (linear charge scale) at mid-loudness level compared to using rectangular pulses (Yip et al., 2017). In summary, previous studies (Ballestero et al., 2015; Navntoft et al., 2020; Yip et al., 2017) suggest some potential advantages with ramped CI pulses but it remains yet to be confirmed with psychophysical data.

In the current study, we present four experiments that provide a detailed investigation of a ramped pulse stimulation paradigm in human CI users. The main goal of the study was to test the hypotheses that (a) ramped pulses provide more efficient electric stimulation than rectangular pulses, (b) a rising ramp is more efficient than a declining ramp, and (c) equally loud ramped pulses will be perceptually discriminable from rectangular ones. In the first experiment, we compared the charge efficiency of ramped and rectangular pulse shapes in terms of detection thresholds with three different stimulation rates and at matched MCLs. In the second experiment, we estimated the loudness growth at 50% dynamic range. In the third experiment, we probed discriminability between the pulse shapes. Finally, in the fourth experiment, we measured thresholds across the electrode array to assess differences quickly in an electrode-to-neuron interface pattern between rectangular and ramped pulses.

General Methods

Subjects

Seven users of an Advanced Bionics™ CI (AB, Valencia, CA, USA) participated in the four experiments. Their demographic information is provided in Table 1. Data were collected in Copenhagen (DK). The research was approved by the Science-Ethics Committee for the Capital Region of Denmark (reference H-16036391). All listeners provided written informed consent prior to participation in the experiment. They were paid for taking part in the study and reimbursed for travel expenses.

Setup

All experiments were conducted using direct stimulation from the implant, bypassing the listener's clinical processor and settings. The setup consisted of an AB Clinical Programming Interface (CPI-2) connected to an AB Platinum Sound Processor (PSP) which was controlled

Table 1. Demographic Details of the Participants.

Demographics							
Subject	Sex	Age (y)	Duration of deafness/severe hearing loss	CI usage (yrs)	Etiology of hearing loss	Implant/electrode[a]	Test ear
S1	F	62	Post-lingual, progressive HL[b] deaf for 15 y	13	Pendred syndrome	HR90 K/HiFocus 1J	L
S2	F	65	Born with severe HL	10	Genetic (inherited)	HR90 K/HiFocus Helix	L
S3	F	69	Born with severe HL	5.5	Rheshus disease	HR90 K Advantage/ HiFocus MS	L
S4	F	39	Born with severe HL	6.5	Genetic (inherited)	HR90 K Advantage/ HiFocus MS	R
S5	F	48	Progressive HL around age of 35	7	Genetic (inherited)	HR90 K Advantage/ HiFocus MS	R
S6	M	51	Progressive HL around age of 28	6	Genetic (inherited)	HR90 K Advantage/ HiFocus MS	L
S7	M	60	Progressive HL around age of 30	6	Meniere	HR90 K Advantage/ HiFocus MS	R

Note. F=female; L= left; M= male; R= right; y= year; yrs= years.
[a]HiFocus 1J: HiFocus™ 1J, 1J: straight lateral wall electrode.
HiFocus Helix: HiFocus™ Helix: pre-curved, peri-modular electrode HiFocus MS: HiFocus™ Mid-Scala, MS: pre-curved, midscalar electrode.
[b]HL: Hearing loss.

using BEDCS software (Bionic Ear Data Collection System, Ver. 1.17.208; AB, Valencia, CA, USA) (Litovsky et al., 2017) and programs written in Matlab (Ver. 2017b; The MathWorks, Natick, MA, US). An older version of AB's Soundwave software (Ver. 1.6.8) was installed on the same laptop to provide an upgraded DLL required to communicate with newer (up to 2017) Advanced Bionics devices than were natively supported by the BEDCS DLL.

Impedance measures were performed for each subject before every test session using AB's Soundwave software (Ver. 3.2.12), installed on another laptop, to calculate maximum current levels within compliance limits (max output of 7–8 vs). Applied current levels did not exceed compliance limits nor safety limit of charge (212 nC per phase; Shannon, 1992). Impedances were also measured at the end of each session to verify that there were no systematic changes after the experiment.

Stimuli

The stimuli consisted of trains of biphasic pulses presented for 500 ms in monopolar electrode configuration (case ground). Each pulse had a duration of 97 μs/phase, no interphase gap, and anodic-first polarity. Three pulse shapes were tested (Figure 1): "Rec," "rampUp," and "rampDown." The rectangular pulse shape (Rec) has, as its name indicates, a rectangular shape with a flat phase amplitude. The two ramped shapes are defined according to their slope (the rate at which the injected current increases or decreases linearly over time) and have a pedestal level or so-called "foot amplitude" (Figure 2a in Ballestero et al., 2015). The assumption is that the pedestal level drives SGNs to subthreshold and the steepness of the slope regulates the evoked firing of SGNs. In rampUp, the slope ramped from a fixed pedestal level at the phase onset to a specified amplitude current level at the phase offset, for both phases. In rampDown, the slope ramped from a specified current amplitude at the phase onset to the fixed pedestal level at the phase offset for both phases. Thus, using rampUp and rampDown we tested the effect of a rising and declining slope, respectively. Based on previous studies using subthreshold stimuli (e.g., Hughes and Stille, 2009), the pedestal level of the ramped pulses was set to 50% of the Rec threshold in μA. The maximum peak current amplitude, and correspondingly, the slope was adjusted to vary the loudness corresponding to the pulse trains.

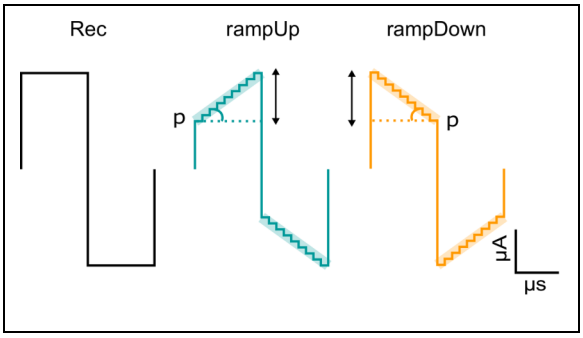

Figure 1. Pulse shapes used. Pulses were charge-balanced, biphasic and anodic-first polarity with 97 μs/phase with no interphase gap. The rectangular pulse shape (Rec) has the standard rectangular shape. In rampUp (green), for both the first and second phases, the slope ramps from a fixed pedestal level (p), set to 50% of the threshold for Rec in μA, at the phase onset to a specified peak current amplitude at the phase offset. In rampDown (orange), for both the first and second phases, the slope ramped from a specified max peak current amplitude at the phase onset to the fixed pedestal level at the phase offset. It means that the pedestal level in rampUp and rampDown is fixed and individualized, while the peak current amplitude (arrow), and thus slope of the ramp, is changed. The slope over one phase was approximated (faded color) in nine steps, each of 10.778 μs duration, due to hardware limitations.

Due to hardware limitations, the amplitude of the pulse was sampled at a rate of 10.778 μs, resulting in slopes encoded by nine samples yielding a total phase duration of 97 μs. Charge per phase for rectangular pulses was calculated as phase duration × peak current amplitude, and for ramped pulses, it was calculated as phase duration × (pedestal level + 0.5 × (peak amplitude current − pedestal level)). The Advanced Bionics implant uses eight bits to encode the intensity of stimulation, which means that, for a given current range, the implant can be stimulated at 256 linear, discrete intensity levels. The minimum achievable step size can be set to 1, 2, 4, or 8 μA allowing for a maximum amplitude of 255, 510, 1,020, or 2,040 μA.

Prior to the experiments, we verified the stimuli with a test implant and a digital storage oscilloscope. Before the measurements, subjects completed loudness ratings for each combination of electrode, presentation rate, and pulse shape. The stimulus current amplitude was gradually increased starting from zero, while listeners indicated the loudness level using a chart that was marked on a scale from 0 ("off") to 10 ("too loud") from AB. Once loudness level 7 ("loud but comfortable") was reached, the stimulus level was reduced until loudness level 6 (MCL) was confirmed.

Statistics

To compare overall effects on threshold, MCL, and angle of the ramp slope (Experiments 1 and 4), factor analyses were performed by using linear mixed-effects models. The models were implemented in R (R Core Team, 2015) using the *lme4* package (Bates et al., 2015). Model selection was performed with the *lmerTest* package (Kuznetsova et al., 2017), using the backward selection approach based on a stepwise deletion of model terms with high p values (Kuznetsova et al., 2015). Normality and homoscedasticity were checked by visually inspecting plots of residuals against fitted values. Post hoc analysis was performed through contrasts of least-square means using the selected lme4 model and *emmeans* library (Lenth et al., 2018;

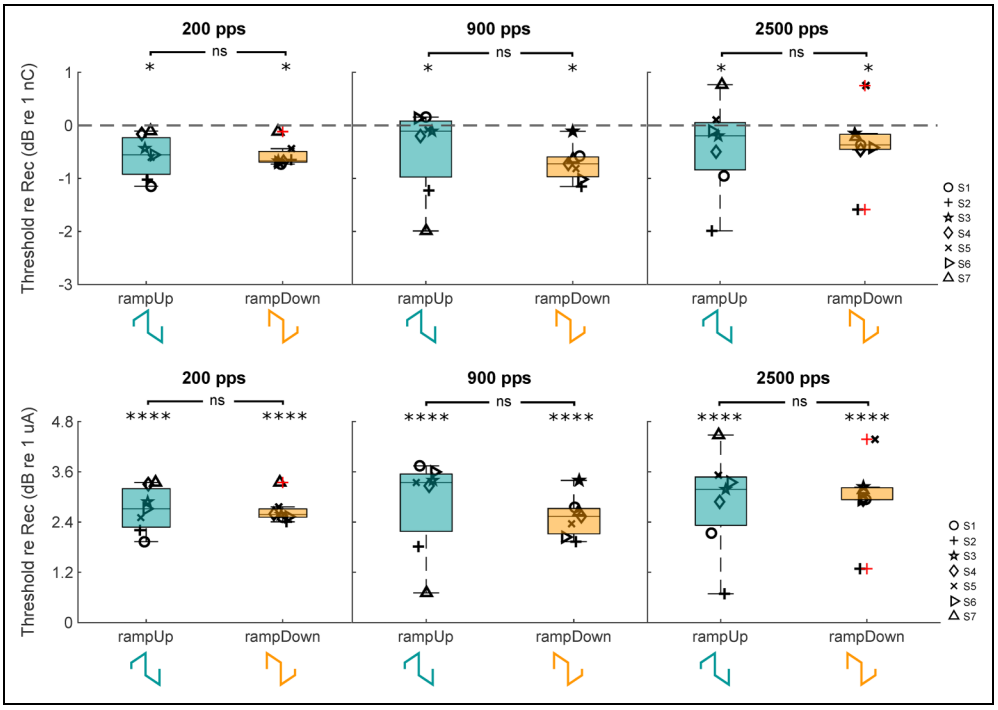

Figure 2. Detection threshold normalized to Rec at three stimulation rates. Left: 200 pps, mid: 900 pps, right: 2,500 pps for Rec (black), rampUp (green) and rampDown (orange) in charge (top row) and in peak current amplitude (bottom row). Negative values indicate lower thresholds relative to Rec. The boxplots represent the distribution of the threshold showing the median, 25th and 75th percentiles, and the most extreme data points. +: individual outliers. Symbols; individual mean threshold. * $p < .05$; **** $p < .0001$.

Searle et al., 1980). p Values were corrected for multiple comparisons using the Tukey method. Significant differences are reported using a significance level of $\alpha = 0.05$. To compare the effect on loudness judgment (Experiment 2) and discriminability (Experiment 3), cumulative binomial probabilities were calculated with a significance level corrected for Type 1 errors using the Bonferroni method. This was done by dividing a significance level of $\alpha = 0.05$ by the number of statistical tests performed.

Experiments

Experiment 1:
Effect of pulse shape on detection threshold and MCLs.

Rationale and Design

The aim was to test the hypotheses that (a) a ramped pulse shape is more charge-efficient than a rectangular one because SGNs respond better to changing inputs than steady-state input and (b) a rising ramped pulse is more charge-efficient than a declining one because a rising ramp delays the activation of KLT, and consequently suppresses firing, whereas KLTs are activated at the onset with a declining ramp. These hypotheses were evaluated by comparing the charge required to produce thresholds and MCLs with rampUp, which has a rising ramp, and rampDown, which has a declining ramp, and Rec pulse shapes. The temporal integration of electric pulses is known to depend on the stimulation rate, as the threshold decreases with increasing rates (Kreft et al., 2004; Shannon, 1989; Skinner et al., 2000; Vandali et al., 2000). The mechanism is linked to central integration of pulses (McKay et al., 2013), facilitation in the auditory nerve, and the fact that a higher stimulation rate quickly gives a neuron additional chances to spike if it had not spiked in response to a previous pulse (Boulet et al., 2016). Without a clear hypothesis, we wanted to explore if a potential effect of pulse shape was dependent on the rate of stimulation. The charge efficiency of ramped pulses was, therefore, first tested at threshold at three stimulation rates, 200, 900 and 2,500 pps, and then at loudness-balanced MCLs at 900 pps, because this rate is commonly used in clinical settings. The pedestal level for rampUp and rampDown was fixed and individualized (based of 50% of the threshold for Rec in μA) (Figure 1), while the maximum amplitude and slope were changed to find the threshold or loudness-balanced level just below MCL.

Methods

Detection thresholds for Rec, rampUp, and rampDown were measured at 200, 900, and 2,500 pps using a

one-up-three-down three-alternative forced-choice procedure (3AFC) (Levitt, 1971). The stimulation was presented on electrode 1, which is the most apical electrode on Advanced Bionics electrode arrays. Intensity levels were varied by adjusting the peak current amplitude. The starting peak current amplitude of every trial was clearly audible. Ten reversals were measured. The first two reversals had a step size of 1 dB followed by eight reversals with a step size of 0.25 dB. The final threshold was calculated as the average of the last six reversal points. Threshold measurements for each pulse shape were repeated three times, yielding a total of 27 measurements (3 stimulation rates × 3 pulse shapes × 3 repetitions). The thresholds for the three pulse shapes were measured in blocks of rates, which were randomized within and across subjects. For each stimulation rate, the threshold for Rec was first obtained (three repetitions). The pedestal level of the ramped pulses was then fixed at 50% of the final Rec threshold in μA for this pulse rate. The thresholds for rampUp and rampDown were hereafter determined in randomized order by changing the peak current amplitude.

Rec, rampUp, and rampDown were loudness-balanced to a loudness at MCL using a two-interval, forced-choice, double-staircase procedure (Jesteadt, 1980). The stimulation was presented on electrode 1 (the most apical electrode.) The first interval contained a stimulus fixed in level (standard); the second interval contained the stimulus to be adjusted (signal). The intervals were separated by a 500-ms interstimulus interval. The stimulation rate was 900 pps. Intensity levels were varied by adjusting the peak current amplitude. Subjects were asked to indicate if the second interval was quieter or louder than the first interval. In two tracks, one starts at a high peak current amplitude (at 0.50 dB above the "most comfortable" level on the AB loudness chart, descending track) and one at a low peak current amplitude (0.50 dB below the "most comfortable" level, ascending track). Eight reversals were used. The peak current amplitude was changed in 0.5 dB steps for the first two reversals and 0.25 dB for the remaining six reversals. Balanced levels were calculated by averaging the last four reversals from both tracks. This procedure (Procedure A) was performed twice, and the average of the obtained signal current level was taken as the matched level. To counterbalance any order bias (Marks & Florentine, 2011), the role of the standard and the signal stimuli were swapped, and the previously matched level was presented as the new standard level. This procedure (Procedure B) was performed twice, and the average of the obtained new signal current level was calculated. The loudness-balanced level of the standard was calculated as the log-transformed average difference in Procedure A (standard) and Procedure B (new signal). Two standard-signal combinations were tested: rampUp-Rec and rampDown-Rec. The test order was randomized within and across subjects. Rec was always the standard in Procedure A. The final loudness-balanced level of Rec was taken as the average between the obtained Rec level in rampUp-Rec and that obtained in rampDown-Rec. The pedestal was fixed at the pedestal level determined in the detection thresholds task for 900 pps, and the peak current amplitude of rampUp and rampDown was varied to find the loudness-balanced level.

Results

Figure 2 (top panel) displays detection thresholds in charge normalized to Rec for 200, 900, and 2,500 pps. Lower thresholds were obtained at faster rates, consistent with previous findings (Kreft et al., 2004; Shannon, 1989; Skinner et al., 2000; Vandali et al., 2000). The figure shows that the charge-savings are similar across rates and that ramped pulse shapes have slightly lower thresholds than Rec. A linear mixed-effects model with stimulation rate (200, 900, and 2,500 pps) and pulse shape (Rec, rampUp, and rampDown) as fixed factors and subject as a random factor reported a significant effect of rate ($F(1,180) = 1{,}385.54$, $p < .0001$) and of shape ($F(2,180) = 4.09$, $p = .0129$) on threshold in charge. The interaction between rate and shape was not significant and was therefore eliminated in the initial step of the model selection. Stimulation rate was entered as a continuous variable with log-transformed rate values because the thresholds as a function of rate followed a straight line on a log, but not linear, scale for most subjects (Figure 3). Post hoc tests with Tukey correction showed that both rampUp and rampDown were significantly different from Rec ($p = .0493$ and $p = .0297$, respectively) and that rampUp and rampDown were not significantly different ($p = .9789$). The charge-savings were −0.50 dB re 1 nC for rampUp and −0.55 dB re 1 nC for rampDown relative to Rec, respectively.

In summary, we hypothesized that ramped pulses are more charge-efficient, that the direction of the slope matters, and that charge-savings with ramped pulses are greater at higher rates. The results support only the first

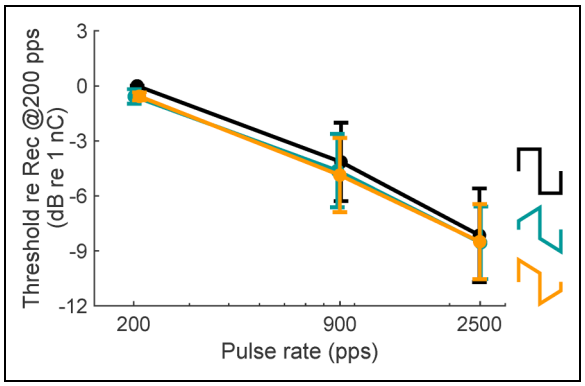

Figure 3. Detection thresholds for Rec (black), rampUp (green), and rampDown (orange) in charge stimulation rate. Data show mean ± SD ($n = 7$).

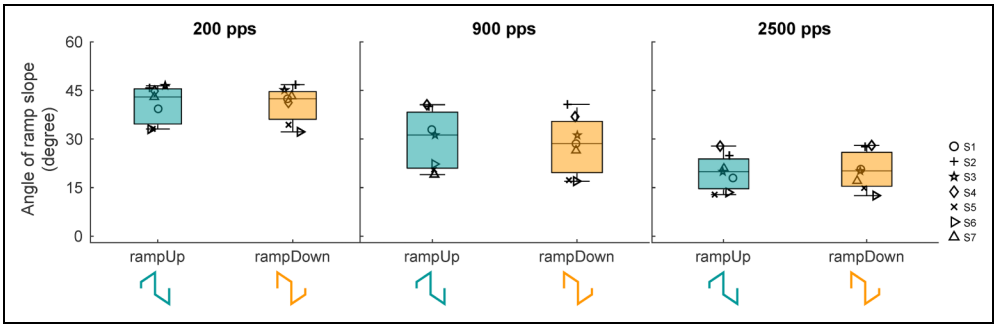

Figure 4. Angle at threshold at three stimulation rates. Left: 200 pps, middle: 900 pps, right: 2,500 pps for rampUp (green) and rampDown (orange). The boxplots represent the distribution of the threshold showing the median, 25th and 75th percentiles, and the most extreme data points. Symbols; individual mean thresholds.

hypothesis. However, as no significant effect could be found for the direction of the slope (rampUp vs. rampDown), or the interaction between the effect of the shape and rate, no conclusion could be made for the latter two hypotheses. The lack of significance between the effect of the shape and rate implies that we cannot discriminate between the slopes of the threshold-rate functions for both Rec, rampUp, and rampDown and that the slope calculated in the statistical model (−3.14 dB re 1 nC per doubling pulse rate) is appropriate for all three pulse shapes. This value is in accordance with function slopes reported in previous studies ranging from −2 to −4 dB/doubling pulse rate depending on rates tested, phase duration, electrode configuration, neural survival, etc. (Kreft et al., 2004; Shannon, 1989; Skinner et al., 2000; Vandali et al., 2000).

The thresholds were also compared in peak current amplitude (in dB) (Figure 2, bottom panel). A linear mixed-effects model fitted to peak current amplitudes, as performed for charge levels, showed a significant effect of both rate ($F(1,180) = 1{,}178.22$, $p < .0001$) and shape ($F(2,180) = 96.44$, $p < .0001$) on the threshold in peak current amplitude. The interaction between rate and shape was not significant and was therefore eliminated in the initial step of the model selection. Post hoc tests with Tukey correction revealed that both rampUp and rampDown were highly significantly different from Rec (both $p < .0001$), while there was no significant difference between rampUp and rampDown ($p = .9533$). The results demonstrate that significantly less charge, but significantly higher peak current amplitude, is needed with ramped pulses at threshold for 200, 900, and 2,500 pps and that the direction of the ramp seems of less importance.

The pedestal level was fixed and individualized (based of 50% of the threshold for Rec in μA), while the peak current amplitude, and thus slope of the ramp, was varied to find the threshold. The steepness of the ramp in a ramped pulse shape is hypothesized to contribute to SGN firing. To investigate this, we calculated the angle of the ramp for rampUp and rampDown at the three stimulation rates. The results displayed in Figure 4 show that the angle was shallower with higher rates. A linear mixed-effects model with stimulation rate and pulse shape (rampUp and rampDown) as fixed factors and subject as random factor reported a highly significant effect of rate ($F(1,117) = 478.44$, $p < .0001$) but not of shape ($F(1,117) = 0.05$, $p = .8154$) or the interaction between rate and shape ($F(1,117) = 0.03$, $p = .8559$) on the angle.

The fact that rampUp and rampDown were similar and that charge-savings with ramped pulses relative to Rec were proportional across rates (similar slope for the threshold-rate) suggests that the shallower angle at higher rates is a consequence of generally lower threshold with higher rates rather than that the angle is a determinant for the threshold.

Figure 5 shows the individual and group loudness-balanced MCL at 900 pps normalized to Rec in charge (Figure 5A) and peak current amplitude (Figure 5B). A linear mixed model showed a significant effect of pulse shape on loudness-balanced levels in charge ($F(2,14) = 22.01$, $p < .0001$). Post hoc comparison with Tukey correction revealed that rampUp and rampDown were significantly lower than Rec ($p < .0001$ and $p = .0008$, respectively), whereas rampUp and rampDown were not significantly different ($p = .2944$). Fitted average values for rampUp and rampDown were 0.78 and 0.59 dB re 1 nC lower than Rec, respectively. There was no significant effect of pulse shape on the difference between threshold and loudness-balanced levels (dynamic range) in charge at 900 pps ($F(2,14) = 1.51$, $p = .2537$).

Comparing loudness-balanced levels in peak current amplitude, shape was again a significant factor ($F(2,14) = 382.93$, $p < .0001$) with rampUp and rampDown being significantly higher than Rec (both $p < .0001$). There was no significant difference between rampUp and rampDown ($p = .3746$). There was a significant effect of pulse shape on the dynamic range in peak current amplitude at 900 pps ($F(2,14) = 12.29$, $p = .0008$). Post hoc analysis reported that the differences for rampUp and rampDown were significantly lower than Rec ($p = .0140$ and $p = .0007$, respectively, Tukey). The results

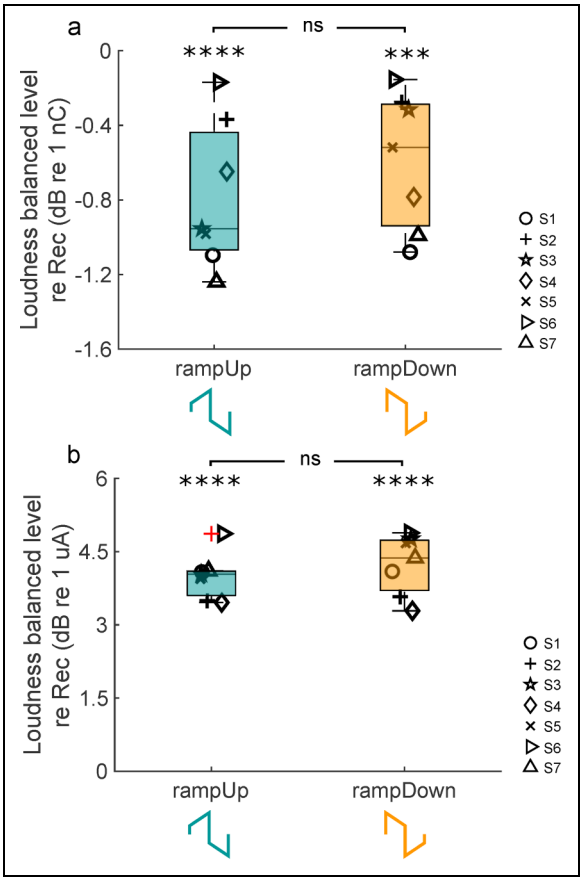

Figure 5. Loudness-balanced just below MCL for Rec (black), rampUp (green) and rampDown (orange) at 900 pps normalized to Rec in charge (A) and in peak current amplitude (B). The boxplots represent the distribution of the threshold showing the median, 25th and 75th percentiles, and the most extreme data points. +: individual outliers. Symbols; individual mean threshold. ** $p < .01$; *** $p < .001$; **** $p < .0001$.

demonstrate (a) that significantly less charge, but higher peak current amplitudes, is needed with ramped pulses at loudness-balanced levels just below MCL, (b) that ramped pulses with slopes of opposite direction yield similar MCLs, and (c) that ramped pulses have similar difference between threshold and loudness-balanced levels as rectangular pulses in terms of charge, but smaller difference between threshold and loudness-balanced levels relative to rectangular pulses in terms of peak current amplitude.

Experiment 2:
Effect of pulse shape on loudness judgment.

Rationale and Design

Even though the three pulse shapes had similar dynamic ranges (Experiment 1), it is plausible that ramped and rectangular pulses produce distinct loudness growth, due to differences in underlying neural activation patterns. The link between neural activation patterns and loudness growth has, for instance, been found in a study probing the effects of polarity (Guérit et al., 2018, 2020; Macherey et al., 2017). The aim of Experiment 2 was to test this hypothesis by comparing the loudness growth function of the three pulse shapes at 50% dynamic range.

Methods

The loudness of Rec, rampUp, and rampDown was compared at 50% of dynamic range using a two-interval forced-choice (2IFC) task. The stimulation was presented on electrode 1 (the most apical electrode). The two intervals contained either Rec and rampUp, Rec and rampDown, or rampUp and rampDown, and subjects were asked to indicate which interval sounded louder. The presentation rate was 900 pps. The pedestal level of rampUp and rampDown was individual and fixed at the pedestal level determined in the detection thresholds task for 900 pps in Experiment 1, and the peak current amplitude of all three pulse shapes was set to 50% of dynamic range (in dB re 1 μA). Each pulse shape combination was presented 32 times, with half of the trials in one order, and the other half with the order swapped, giving a total of 96 trials. The combination order was randomized within and across subjects.

Results

Figure 6 displays the results for the loudness judgment task. The figure is a stacked bar graph where the size of the color bar indicates the percentage to which the pulse shape was judged as loudest in the given combination of two pulse shapes. The bar order is arbitrary. The dashed lines denote the upper and lower confidence interval of the level of chance. Thus, non-significant bar sizes mean that subjects could not detect a difference between the loudness of the two pulse shapes at 50% dynamic range, consistent with a proportional growth of loudness. The judgments varied between subjects. For instance, S3, S4, and S5 judged that Rec in combination with either rampUp or rampDown sounded equally loud. S2 and S7 reported in contrast that Rec sounded louder than the ramped pulse shapes. Half of the subjects (S2, S3, S4, and S5) judged that rampUp and rampDown sounded similarly loud while the reports of the other half were mixed. In summary, there was no overall clear difference in the loudness judgment at 50% dynamic range between the three pulse shapes. The complete loudness growth functions may be needed to determine the effects of ramped pulse shapes on loudness.

Experiment 3:
Discrimination between pulse shapes

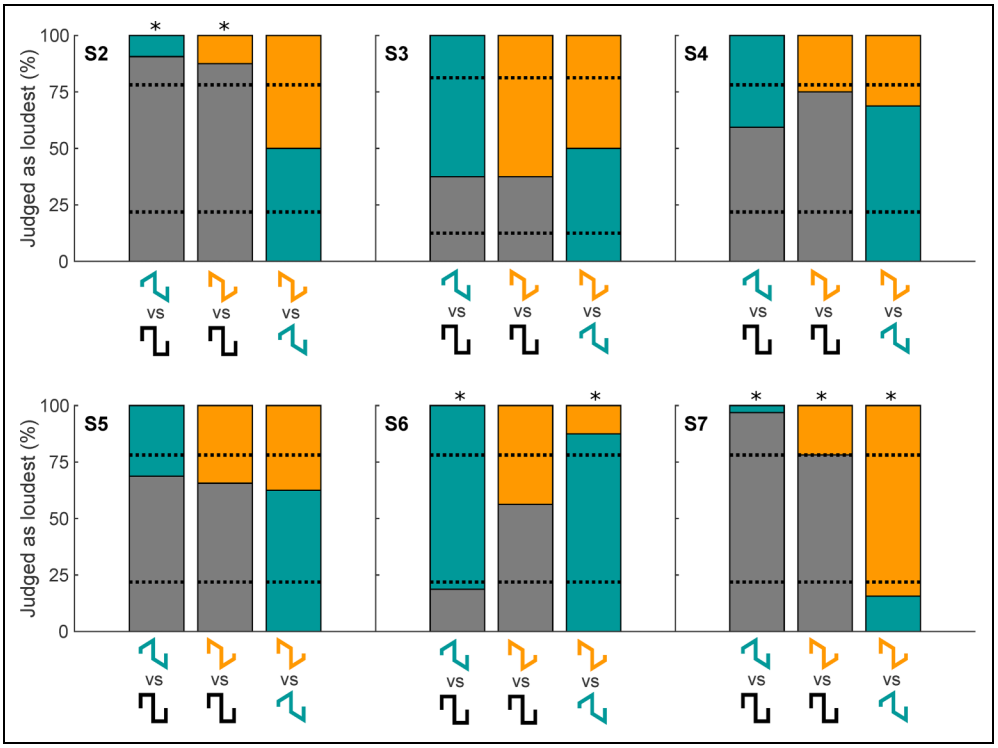

Figure 6. Loudness judgment at 50% dynamic range for each combination of two pulse shapes. Rec (black bar), rampUp (green bar), and rampDown (orange bar). The bar order is arbitrary. The size of the color bar indicates the degree to which the pulse shape was judged as loudest in the given combination in percentage. Dashed lines denote the upper and lower confidence interval of 50% chance with $\alpha = 0.05$. * a cumulative binomial probability $P(x \leq X)$ above $\alpha = 0.0024$ (using Bonferroni correction for Type I errors) denotes a significant difference.

Rationale and Design

If ramped pulses provide a more focused activation of the auditory nerve, they might be perceived differently than rectangular pulses (Landsberger et al., 2012). The aim of Experiment 3 was to examine this hypothesis using a discrimination task. Three equally loud stimuli were presented on the most apical electrode (electrode 1). Two of the stimuli had the same pulse shape. Subjects had to identify which stimulus was different in any way other than loudness. We chose this coarse task over more specific ones, such as pitch discrimination or sound quality scaling (Landsberger et al., 2016), because general discriminability of ramped pulses had not been examined before. The level of the sounds was the loudness-balanced levels at MCL obtained in Experiment 1 with a level jitter to prevent loudness cues. The individual and fixed pedestal levels were those determined in Experiment 1 for 900 pps.

Methods

Discrimination between the three pulse shapes was tested in a three-interval forced-choice (3IFC) task. One randomly selected interval contained the target pulse shape, while the two other intervals contained the same non-target shape. The inter-stimuli-interval was 500 ms, and the stimulation rate was 900 pps. The subject was asked to identify which interval was different in any way other than loudness. Subjects did not report what cues they used for the discrimination task. The pedestal level of rampUp and rampDown was fixed at the pedestal level determined in the detection thresholds task for 900 pps, and the peak current amplitude of the three pulse shapes was the loudness-balanced levels. To prevent identification based on any small residual loudness difference after the loudness balancing, a random level rove was added in each interval. The amplitude of the "level jitter" was randomly selected in an interval ranging from −4.5 to 4.5 times individual standard error obtained in the loudness balancing task (2.3*1.96*SE as discussed in Fraser and McKay, 2012). This amount of jitter, shown in Table 2, ensured that the variation of loudness was greater than the possible error in loudness matching (Dai & Micheyl, 2010).

To familiarize the subjects with the task, we first performed a "Single combinations"-session with three pulse-shape combinations: Rec-rampUp, Rec-rampDown, and rampUp-rampDown ("Single combinations" in Table 3). Each combination was presented successively in 30–40 trials (in blocks of 10 trials) for Rec-rampUp and Rec-rampDown, and in 60–80 trials for rampUp-rampDown. If the subject was able to significantly discriminate between the pulse shapes in the "Single

Table 2. Level Roving Used in the Discrimination Task Expressed in dB re 1 μA.

Level roving used in discrimination task (dB re 1 μA)			
Subject	Rec	rampUp	rampDown
S1	0.50	0.41	0.47
S2	0.45	0.55	0.50
S3	0.65	0.69	0.45
S4	0.65	0.69	0.45
S5	0.61	1.01	1.15
S6	0.52	0.43	0.42
S7	0.40	0.45	0.59

combination"-session, defined as a score with a p value below .05 (see "Statistics" in General Methods), then the subject continued with a "Mixed combinations"-session ("Mixed combinations" in Table 3). Here, the combination of pulse shapes changed from trial to trial, thus making the task harder. Fifty to sixty trials of the "Mixed combinations"-session were performed. Feedback was provided in both sessions.

Results

Table 3 shows the results of the discrimination task. The number of correct trials (#CorrTrials) out of the number of trials presented and the corresponding p value calculated from cumulative binomial probability ($P(x \leq X)$) are displayed. A significant probability value on the group level is marked blue. Only one subject, S6, could reliably discriminate between rectangular and ramped pulse shapes when presented in both the single and mixed combination conditions on the group level. Worth noticing is the fact that this subject had the shortest duration of deafness (Table 1). See Table 3 for more details on the results from the other subjects.

Experiment 4:
Effect of pulse shape on threshold profiles

Rationale and Design

Variability in thresholds across the electrode array has been used to examine spatial selectivity of various electrode configurations (Bierer, 2007; Bierer & Faulkner, 2010; Bierer & Nye, 2014; Long et al., 2014; Marozeau et al., 2015) and to deactivate high-threshold electrodes (Bierer & Litvak, 2016). The rationale is that regions along the array with poor electrode-to-neuron interface have high thresholds due to low efficiency with which excitation changes are encoded in SGNs, placement of electrodes further away from the SGNs (Skinner et al., 2002), loss of SGNs, varying tissue impedances (Vanpoucke et al., 2004), or other factors. In contrast, regions with good electrode-to-neuron interface have relatively low thresholds. This is consistent with the idea that pathology is uneven along the tonotopic axis (Nadol, 1997). A stimulation paradigm that provides focused activation is thought to be able to capture this irregularity resulting in high channel-to-channel variability. For instance, tripolar or multipolar mode, which generates a relatively narrow area of excitation, results in more variable thresholds along the electrode array. In contrast, monopolar mode, with a relatively broad electric field, activates distant neurons with a small current increase, which eventually lead to less variability in thresholds across the electrode array (Bierer & Faulkner, 2010; Bierer & Nye, 2014; Marozeau et al., 2015). While there are many factors that can affect threshold profiles, all relevant factors other than pulse-shape remain constant. Specifically, electrode-modiolus distance, number of surviving fibers, tissue impedance, and stimulation mode remain constant across conditions. Therefore, we expect any observed

Table 3. Results of the Discrimination Task.

Discrimination task								
	Single combinations						Mixed combinations	
Subject	rampUp [a]CorrTrials	Rec $P(x \leq X)$	rampDown [a]CorrTrials	Rec $P(x \leq X)$	rampUp [a]CorrTrials	rampDown $P(x \leq X)$	[a]CorrTrials	$P(x \leq X)$
1	17/40	0.1343	15/40	0.3257	26/80	0.6041	-	-
2	8/20	0.3385	6/20	0.7028	-	-	-	-
3	8/30	0.8332	16/30	0.0188	25/30	< 0.0001	20/50	0.1964
4	9/30	0.7007	9/30	0.7007	-	-	-	-
5	16/30	0.0170	15/30	0.0399	30/60	0.0056	26/60	0.0680
6	14/20	0.0008	22/30	< 0.0001	13/30	0.1563	18/30	0.0022
7	14/40	0.4703	22/40	0.0039	29/80	0.3281	24/60	0.1685

[a]CorrTrials denotes the number of correct trials out of the number of trials presented, and $P(x \leq X)$ the corresponding p value calculated from cumulative binominal probability. Red text denotes a significant probability value for individual subjects with $\alpha = 0.05$, and blue text denotes a significant probability value for the group level with $\alpha = 0.0022$ (using Bonferroni correction for Type 1 errors).

differences in threshold profiles would reflect a difference in neural activation induced by the pulse shape. To assess this difference, fixed pedestal levels were individually determined in a preceding experiment, except for S4 (see Methods), and the peak current amplitude, and thus slope, was varied to find the threshold.

Methods

Threshold profiles were measured along the array on all odd numbered electrodes (1, 3, 5, 7, … 15), one electrode at a time, using an adaptive one-up/one-down tracking procedure, as done in Goehring et al. (2019). To save time, we choose not to use a 3AFC task as in Experiment 1. Instead, the subject was asked to press Enter on the computer keyboard each time a sound was heard. Intensity levels were varied by adjusting the peak current amplitude. If the subject responded to the stimuli within a time window of 3 s (a hit), the peak current amplitude was decreased by one step size and a new stimulus was presented after a randomly chosen delay between 2 and 3 s. If the subject did not respond within 3 s after the stimuli (a miss), the level was increased by one step size and presented after a randomly chosen delay of between 0.1 and 0.6 s. False alarm detections during this delay had no consequences. This resulted in a stimulus presentation every 2–6 s. Eight reversals were used, two with a step size of 1 dB, followed by six with a step size of 0.25 dB. The threshold level was the average of the last four reversal points, and the final threshold was averaged over the two repetitions for each pulse shape.

Similar to the 3AFC detection thresholds task in Experiment 1, the threshold for Rec was first measured on each electrode with two repetitions per electrode, yielding 16 measurements (1 shape × 8 electrodes × 2 repetitions). The electrode test order was randomized within and across subjects. The pedestal level of the ramped pulses was then fixed at 50% of the obtained Rec threshold (in μA). Hereafter, the thresholds for Rec, rampUp, and rampDown were determined on one electrode at a time by varying the peak current amplitude. Each pulse shape was repeated twice per electrode, giving 48 measurements (3 shapes × 8 electrodes × 2 repetitions). We chose to include Rec again in the randomized run with the ramped pulses to prevent any order effect. The final threshold estimates for each pulse shape were the average of the two runs in the randomized run for that pulse shape. The electrode test order and the pulse shape order on each electrode were both randomized within and across subjects. The starting point of every trial was clearly audible.

The procedure for S4 and S2 was slightly different. S4 was the first subject to perform the experiment. In the initial protocol, on one electrode at a time, Rec was first presented twice (to obtain the pedestal current level) followed by the randomized presentation of rampUp and rampDown, giving 48 measurements (3 shapes × 8 electrodes × 2 repetitions). To avoid any order effects in the following subjects, the protocol was changed to include two initial measurements of Rec per electrode to determine the pedestal level such that three pulse shapes could be randomly presented, as described above. S2 perceived echoes with an inter-stimulus interval of 2–6 s, which complicated the threshold detection. To minimize this problem, inter-stimuli-interval was increased to 4–8 s, which reduced the perceived echoes.

Results

Figure 7 shows individual threshold profiles for Rec, rampUp, and rampDown in charge. Tested electrodes are numbered from 1 to 15 with 1 being the most apical electrode. The curves for the three pulse shapes were overall very similar, indicating no apparent difference between the pulse shapes in terms of channel-to-channel variability. The channel-to-channel variability was further quantified as the absolute difference in thresholds across electrodes. To calculate this, the threshold of one electrode was subtracted from the average threshold of that electrode and the two flanking ones. The absolute differences were summed across the array, as done for the "Harmonic spectral deviation measures" in (Peeters et al., 2011). Electrodes at the edges only contributed to the analysis as flanking electrodes. The calculated threshold variabilities in charge are displayed in Figure 8. The three pulse shapes produced similar variability, which is consistent with the lack of significant effect of the factor shape ($F(2,12) = 0.13$, $p = .8800$) on the variability in a mixed-effects linear model with subject entered as a random factor.

These observations contrast with the hypothesis of a distinct neural activation pattern with ramped pulses compared to rectangular pulses. One possible explanation could be that the broad, monopolar configuration used overrules a potential difference with a ramped pulse shape, which is elaborated on in the Discussion section.

Figure 9A,B shows the threshold normalized to Rec averaged across all electrodes in charge and peak current amplitude, respectively. RampUp and rampDown had lower thresholds in charge compared to Rec for all subjects, except S4. A linear mixed-effects model with pulse shape and run as fixed factor and subject as random factor reported non-significant effects of both shape ($F(2,305) = 1.28$, $p = .2799$), run ($F(2,305) = 0.73$, $p = .3942$) and the interaction between shape and run ($F(2,305) = 0.07$, $p = .9323$) on the threshold in charge. The statistical model predicted averaged charge-saving across the electrodes to be −0.26 dB re 1 nC for both rampUp and rampDown relative to Rec. A similar mixed-effects model reported a significant effect of shape on the threshold in peak amplitude current ($F(2,305) = 99.08$, $p < .0001$). Run and the interaction between shape and run were not significant and were therefore eliminated in the initial step of the model selection. Post hoc tests with Tukey correction demonstrated that rampUp and rampDown were significantly different than Rec ($p < .0001$ for both comparisons), and that rampUp and rampDown were not significantly different ($p = .9979$). The statistical model predicted averaged peak current amplitude-increases across the electrodes to be

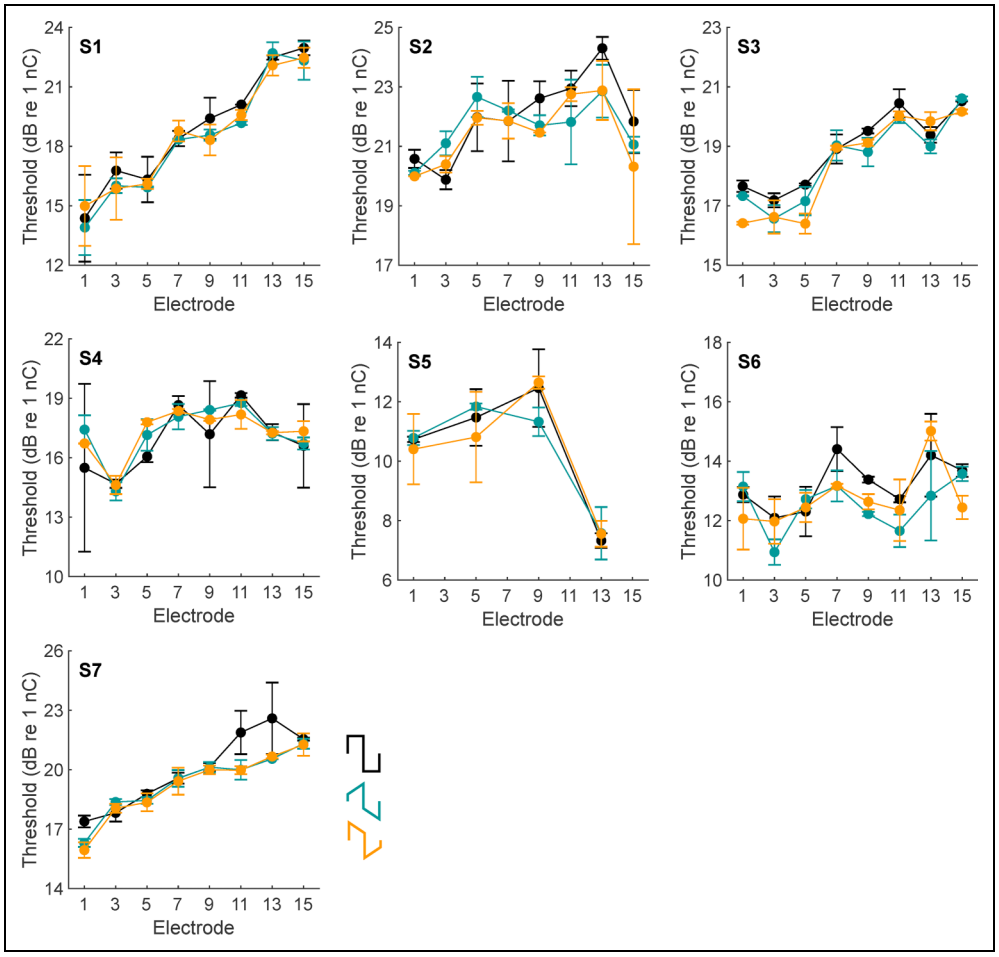

Figure 7. Individual detection thresholds in charge across the electrode array for Rec (black), rampUp (green), and rampDown (orange). Electrode 1 is the most apical electrode. Data shows the mean ± SD. S, subject.

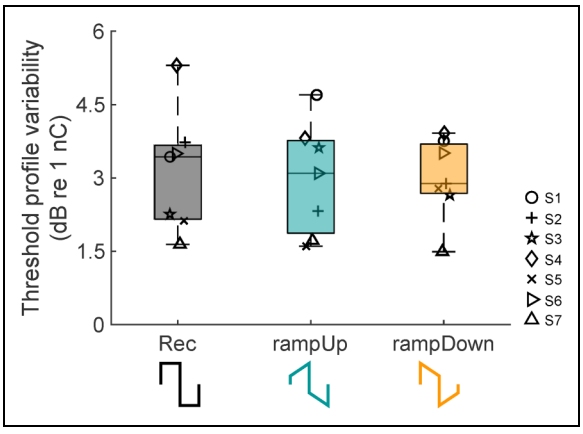

Figure 8. Variability in threshold profile quantified as the sum of absolute difference in threshold across the array for Rec (black), rampUp (green), and rampDown (orange). Electrodes at the edges were not included. The boxplots represent the distribution of the sum of absolute difference in threshold across the array showing the median, 25th and 75th percentiles, and the most extreme data points. Symbols; individual mean threshold.

+3.10 and +3.08 dB re 1 μA for rampUp and rampDown relative to Rec, respectively.

Thresholds in charge were significantly lower with ramped pulses relative to rectangular pulses on the most apical electrode in Experiment 1 (Figure 2, top panel), but not across the array in this experiment (Figure 9A). Thresholds on the most apical electrode in the threshold profile task were therefore compared to those obtained using the 3AFC procedure in Experiment 1 to test if this discrepancy was due to the differences in methodology. A linear mixed-effects model with method (3AFC, Threshold Profiles) and pulse shape as fixed factor and subject as random factor reported non-significant effects of both method ($F(1,93) = 1.98$, $p = .1622$), shape ($F(2,93) = 2.20$, $p = .1164$) and the interaction between method and shape ($F(2,93) = 0.20$, $p = .8196$) on the threshold in charge.

In summary, a ramped pulse (a) did not exhibit a more variable threshold profile, suggesting similar neural activation pattern, and (b) showed non-significant charge-savings, but significant peak current increases, across the array

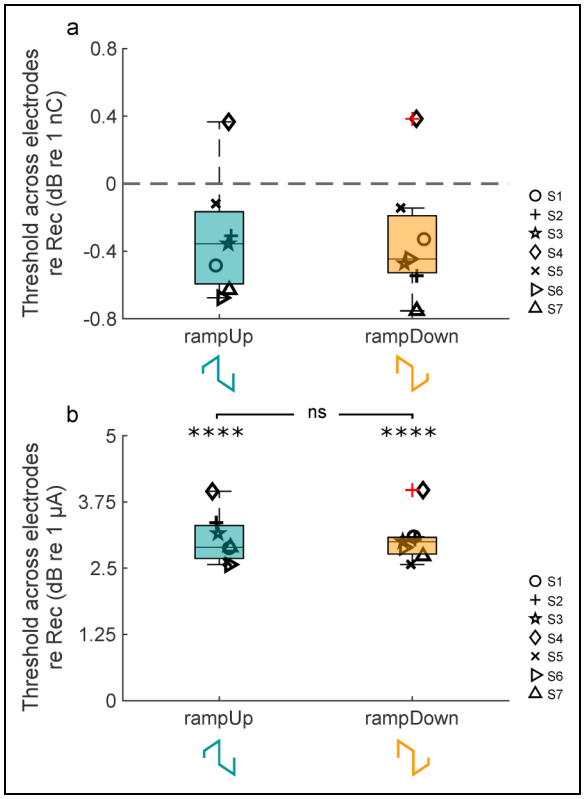

Figure 9. Detection thresholds for Rec (black), rampUp (green), and rampDown (orange) averaged across all electrodes and normalized to Rec in charge (a) and in peak current amplitude (b). The boxplots represent the distribution of the threshold showing the median, 25th and 75th percentiles, and the most extreme data points. +: individual outliers. Symbols; individual mean threshold. **** $p < .0001$.

compared to a rectangular pulse. However, thresholds on the most apical electrode were not significantly different from those obtained using the 3AFC in Experiment 1.

Discussion

This study tested the hypothesis that a pulse shape with a ramped slope would provide greater charge efficiency and a distinct neural activation pattern than a rectangular pulse shape. The results show statistically lower charge with rampUp at loudness-balanced levels (Figure 5) and at threshold across three stimulation rates on the most apical electrode (Figure 2), but not across the electrode array (Figure 10) compared to Rec. However, rampUp was not statistically different from rampDown across all tests suggesting that the direction of the ramp is of less importance. The threshold profile task showed that ramped and Rec pulses had similar profiles and channel-to-channel variability, suggesting comparable neural activation patterns (Figures 7 and 8). Nonetheless, one subject could reliably discriminate between the three pulse shapes (Table 3), suggesting that there might be (small) differences in neural responses between the pulse shapes in this subject.

Clinical Relevance of Charge-Savings and Implications for Power Consumption

Charge-savings with ramped pulses were ~0.4 dB re 1 nC for thresholds and ~0.7 dB re 1 nC for loudness-balanced levels at MCL (Experiments 1 and 4). This would correspond to a shift in dynamic range in terms of charge. One way to evaluate the relevance of the charge-savings in a clinical setup is to calculate the shift in clinical units (CU) (Experiment 1: 15.4 dB re 1 nC for Rec and 14.8 dB re 1 nC for ramped pulses for thresholds at 900 pps, and 22.5 dB re 1 nC for Rec and 21.9 dB re 1 nC for ramped pulses for the loudness-balanced levels). The CU-system used by Advanced Bionics is charge-based with a CU maximum output of 6,000 and the T-level set to 1/10 of the M-level. Using the formula with amplitude × phase duration × k, where k = an arbitrary scaling constant .013 (Advanced Bionics, 2010), then the charge-savings with ramped pulses at thresholds and at loudness-balanced levels are equal to 6 CU and 11 CU, respectively. The M-level is, on average, around 180 CU in most AB users after some experience with the implant. Ninety percent of AB users are estimated to have M-levels below 300 CU (personal correspondence with Advanced Bionics). The saving of 11 CU with ramped pulses therefore corresponds to a reduction of 6% with average M-levels and

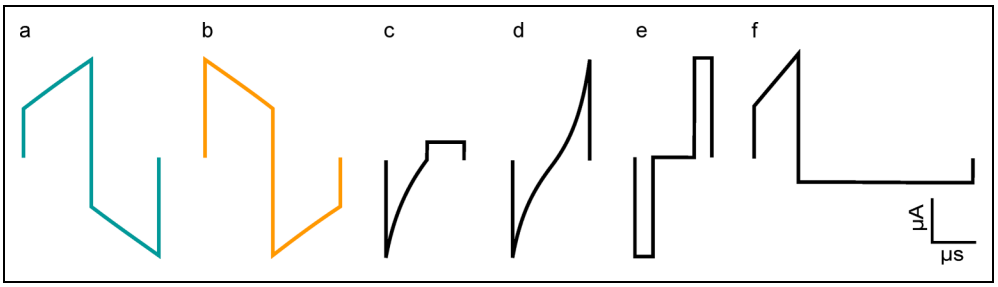

Figure 10. Pulse shapes. (a) rampUp and (b) rampDown used in this study. (c) The genetic-algorithm generated pulse shape and (d) the pulse shape tested in human CI users in Yip et al. (2017). (e) The pulse shape with a long interphase gap. (f) A pseudomonophasic pulse shape with a ramped short duration-high amplitude phase and a long duration-low amplitude phase for charge-balance.

a reduction of 4% with M-levels in the highest quantiles (90%) of AB users.

One potential implication of lowering thresholds and MCLs is the possibility to reduce power consumption in CIs. Power savings may enable implementation of more battery-hungry stimulation strategies, increase battery life, or provide the opportunity to reduce the size of the battery. Given that the battery components are the largest part of CI sound processors, reducing the size of the batteries is critical to meet the market demand for smaller processors. Similarly, to produce a fully implantable CI, the batteries must be included as a part of the internal component and cannot easily be replaced. As such, reducing power consumption requirements are a key component for fully implantable CI development. Power is given by electrode impedance multiplied by current squared ($P = R * I^2$) and charge is given by current over time ($C = I * dt$). This means that ramped pulses, found to be more charge-efficient, are more power-efficient compared to rectangular pulses.

At present, most power is consumed by the RF link, which with an efficiency of around 30% delivers approximately 15% of the total power to the internal part of the device (personal correspondence with Advanced Bionics). Power-requiring tasks of the implant include decoding the radio-frequency link, power supply of the current source(s) and amplifier for impedance recordings, various housekeeping tasks, etc., in addition to stimulation delivery. Although the stimulation delivery is a relatively small part of the total power budget, ramped pulses might still provide a power benefit of a clinically relevant magnitude. Future studies quantifying power consumption with a stimulation strategy using ramped pulses, processing for instance speech material, are needed to verify this.

Finally, the maximum current amplitude deliverable by an implant is determined by compliance voltage of the current source and electrode impedance. Thus, despite the fact that ramped pulses are more charge-efficient, the higher peak current amplitude needed might be a disadvantage in terms of compliance limits.

The Effect of a Ramped Slope and the Pedestal Level

The data support the hypothesis that ramped pulses are more charge-efficient than rectangular ones, but not that ramped pulses with a rising slope are more charge-efficient than with a declining ramped slope. One possible factor that needs to be considered for the latter is the pedestal level. It was defined as 50% of the rectangular pulse at threshold (in μA) but it is likely not optimal. Thresholds were measured in a perceptual task but how this level relates to the thresholds of auditory nerve fibers in each subject is not fully understood. It has been suggested that in the impaired ear, psychophysiological detection thresholds may be reached with only one or a few auditory nerve fibers (Shannon, 1985). Given that human subjects can detect a tactile stimulus that generates a single action potential on a single cutaneous peripheral nerve fiber (Vallbo & Johansson, 1976), this assumption seems reasonable. This possibility is consistent with the finding that psychophysical detection thresholds were very similar to minimum neuronal response thresholds in the inferior colliculus of implanted cats (Beitel et al., 2000). One could, therefore, argue that the pedestal level used might be too low to have an effect, which might explain why no differences were detected between rampUp and rampDown. Also, more work on KLT channels and their voltage-dependent time constants is needed to know if these play a role in the lack of difference observed between rampUp and rampDown. Furthermore, the data in Figure 4 do not clarify whether thresholds are determined by a specified amount of charge delivered (decrease in charge with ramped pulses was proportional to that of Rec across rates), by a specific angle of the ramped slope independently of direction, or if the shallower angle is a consequence of lower threshold with higher rates. Future experiments using ramped pulses with opposite slope directions and fixed/varying pedestal levels combined with varying/fixed angle values are needed to understand the contribution of these parameters to SGN excitability and how this relates to responses at both neurophysiological and perceptual levels.

A significant effect of pulse shape was found on thresholds on the most apical electrode (Experiment 1) but not across the array (Experiment 4). However, the thresholds in charge on the most apical electrode measured by the two methods were not significantly different, suggesting that the results are not necessarily conflicting. Statistical power and noisy data might be two competing factors involved. More data was collected in Experiment 4, suggesting increased statistical power. However, the methodology used in Experiment 4 was optimized to be time efficient as thresholds measurements needed to be repeated across multiple electrodes. It may very well be that as a result of the faster procedure, the threshold measurements in Experiment 4 may be noisier than the thresholds measured in Experiment 1. However, there are not enough repetitions in Experiment 4 to quantify differences in threshold measurement variability. Run was not a significant factor in the threshold profile task, which implies no systematic effect of time. Furthermore, it is worth pointing out that Experiment 4 was designed to quickly probe differences in neural activation at threshold and not charge-savings per se. Another potential explanation for the discrepancy between the results in the two experiments is related to neural survival. Shapes on the most apical electrode are compared across the same neural density around that electrode, while shapes are compared across a heterogeneous neural survival pattern along the cochlea in the threshold profile task. This may result in that some electrodes show an effect of a ramped pulse relative to a rectangular one, and some might not, but that these effects are overall too small to observe a significant difference between shapes. This explanation is

not necessarily inconsistent with the hypothesis of more efficient stimulation with ramped pulses.

Comparison with Previous Studies on Ramped Pulses

Yip et al. (2017) found that an exponential pulse shape resulted in charge-savings of 12.6 nC at midlevel loudness, corresponding to 2.6 dB re 1 nC compared to a rectangular pulse. This exponential shape had a 54-μs phase duration, made of five time steps, with cathodic-first polarity presented on a mid-array electrode in an unreported electrode configuration (Figure 10D), whereas we used a 97-μs phase duration, composed of nine time steps, with anodic-first polarity presented on the most apical electrode in monopolar mode (Figure 10A,B). We chose a longer pulse duration to get a smoother ramp (more time steps) and to include a pedestal level to drive neurons to subthreshold. A direct comparison between the linearly ramping shape used in this study and the exponentially ramped shape used in Yip et al. is therefore not straightforward due to different stimulation parameters tested. However, one explanation for the larger effect observed by Yip et al. could be that an exponentially ramped shape is simply more charge-efficient than the linearly ramping shapes used with rampUp and rampDown, possibly because the auditory system, and biology in general, operate on non-linear scales (Carney & McDonough, 2019). Another possible explanation is related to the notion that the neural membrane is a "leaky integrator," which means that more charge is needed to compensate membrane leakage with longer than shorter pulse durations in order to excite a neural response (Parkins & Colombo, 1987; Shepherd & Javel, 1999). It might therefore be that the effect of a rising ramped shape is reduced by leaky integration during the 97 μs/phase pulse which is less of an issue with approximately half the phase duration used in Yip et al. However, if this was the case, then we would have expected to see differences between rampUp and rampDown. Finally, it is known that increasing the interphase gap reduces behavioral and physiological thresholds (Carlyon et al., 2005; Miller et al., 1999; Shepherd & Javel, 1999; Van Wieringen et al., 2005). It could therefore be that the exponential phase with a time constant of 25 μs (Yip et al., 2017) is equivalent to a longer interphase gap (Figure 10E), which would also result in charge-savings.

The present results are not fully consistent with our recent study on ramped pulses using eABR in CI-implanted mice (Navntoft et al., 2020). Less charge, but higher peak current amplitude, was needed to evoke eABR responses with ramped shapes that were similar in amplitude to responses with rectangular shapes (Navntoft et al., 2020). In contrast to the human data, the animal data showed that the most charge-efficient pulse shape had a rising ramp over both phases (rampUp), supporting the hypothesis of sensitivity to rising current input. The discrepancy between the two studies could be due to the potential suboptimal pedestal level used in the human, but not animal, study, discussed above. It could also be due to the following differences between mice and human, as also highlighted in (Navntoft et al., 2020). First, human auditory nerve fibers are less myelinated with longer peripheral processes and larger fiber diameters. As a consequence, humans have higher membrane capacitance meaning that relatively more energy is required to initiate an action potential compared to mice. Second, SGN loss in the human subjects is likely worse than in the acutely deafened mice. Therefore, ramped pulses might reach healthy fibers and evoke action potentials with less charge in mice, whereas a potential ramp-sensitivity "drowns" in current spread associated with more pronounced neural degeneration, and consequently larger electrode-to-neuron distance, in human. It is indeed possible that the effectiveness of ramped pulses and the ability to discriminate ramped pulse shapes is dependent on the quality of the electrode–neural interface. New data is required to evaluate this possibility. However, it is worth noting that the only subject who was able to discriminate between pulse shapes was also the patient with the shortest duration of deafness. Furthermore, based on conversations, the three participants with congenital hearing loss and implanted as adults had poorer speech perception than the other, and two of them could also not discriminate between pulse shapes. These observations are at least consistent with the possibility of dependence on electrode–neural interface on pulse shape discrimination.

Third, the animal recordings were performed on an electrode in the basal part of the region, which expresses a greater density of ramp-sensitive KLT ion channels compared to the apical part of the mouse cochlea (Adamson et al., 2002), while the human responses in Experiments 1–3 were obtained on the most apical electrode placed in the apical-mid region (the average insertion angle of the 1J electrode array is 405 degrees (Landsberger et al., 2015). Nonetheless, if this was the case, then we would have expected a larger difference in thresholds between apical and basal electrodes in the threshold profile task, which was not the case (Figure 7). Fourth, the discrepancy between the animal and human findings could also be due to the pulse shape parameters used; a pulse train with a phase duration of 97 μs/phase, no interphase gap, and a pedestal level were used in this study, while single pulses with a phase duration 25 μs/phase, 10 μs interphase gap, and no pedestal level (triangular shape ramping from 0 μA to a specified current) were presented at much slower rate (23 pps vs. 200/900/2,500 pps) in the animal study. Apart from the note on phase duration and leaky integration discussed above, it could be that a triangular shape is more efficient than the ramped shape with a fixed pedestal level. Finally, the human behavioral response reflects several steps of processing along the auditory pathway, including the integration of temporal and spatial information and cognitive factors, compared to the gross measure of neural activity obtained with

eABRs, which reflects synchronous activity of low-threshold fibers.

A study by Dobie and Dillier investigated discrimination between triangular, trapezoidal, and rectangular pulses in two patients with a single extracochlear electrode and an analog stimulation paradigm (Dobie & Dillier, 1985). They found that rise-times (for 0 to maximum current) as low as 80 μs could be discriminated. Although the electrode placement and temporal parameters are different, this supports our findings that discrimination between rising or declining ramps and rectangular pulse shapes is possible (Experiment 3). Interestingly, the authors suggested that the degree of synchrony among a population of auditory nerve units may provide the neural cue for pulse shape discrimination. This neuronal population consists of low, medium, and high spontaneous rate fibers that differ both in their type of synapse with the inner hair cells and with respect to anatomy and spatial arrangement (Kawase & Liberman, 1992; Leake et al., 1993; Liberman, 1980, 1982; Liberman & Oliver, 1984; Merchan-Perez & Liberman, 1996). If low, medium, and high spontaneous rate fibers have different threshold for firing an action potential, then they will fire at the same time for the rectangular waveform but at different time points in the triangular waveform. Thus, low-threshold fibers may fire slightly earlier than high-threshold ones at a particular point on the rising ramp in a triangular waveform. The outcome is less phase-locking across fibers with triangular than rectangular waveforms (see Figure 9 in that paper). Finally, Dobie and Dillier also found that less charge was needed with triangular pulses to reach MCLs compared to rectangular pulses in one listener, as found in this study (Experiment 1). There was no effect of pulse shape on charge consumption in the other listener (Dobie & Dillier, 1985).

As a final note, the two phases in a biphasic pulse interact in a complex way (Joshi et al., 2017a). Future research could therefore be directed at testing the effect of a single ramped phase in human CI users or animals using a pseudomonophasic pulse shape with a ramped short duration-high amplitude phase and a long duration-low amplitude phase for charge-balance (Figure 10F), instead of two ramping phases of equal phase duration and amplitude used in this study (Figure 10A,B), in order to get a better understanding of the effect of a single ramped slope.

Conclusion

In this study, a novel non-rectangular stimulation paradigm with a ramped pulse shape was compared to the standard rectangular pulse shape in CI listeners on charge efficiency, discriminability, and threshold profiles across electrodes in monopolar mode. Major findings include:

1. Less charge, but higher peak current amplitude, is needed at threshold and MCLs with a ramped compared to a rectangular pulse. Charge-savings were around 0.4–0.7 dB re 1 nC and were less pronounced than threshold differences across stimulation rates. The latter does not support the hypothesis that ramped pulses are more efficient at high compared to low stimulation rates.
2. No significant difference was found between a rising and declining ramped pulse shape, suggesting that the direction of the ramp has a relatively little effect.
3. One out of seven subjects could reliably discriminate between equally loud ramped and rectangular pulses.
4. Ramped and rectangular pulses produce similar threshold profile.
5. Findings were generally consistent with the hypothesis of ramped slopes providing increased charge efficiency. The effect sizes would correspond to charge-savings of 6% with an average M-level in a clinical setting.

Acknowledgments

We would like to thank our subjects for their dedicated and diligent participation. We would also like to thank Francois Guerit, Cambridge University, England, for providing help on the Advanced Bionics hardware and setup. This work was supported by a grant from the Swiss National Science Foundation (ERC transfer grant to T.R.B.) and William Demant Foundation (partial salary of C.A.N). The funder did not have additional role in the study design, data collection and analysis, decision to publish, or preparation of the manuscript.

Declaration of Conflicting Interests

The author(s) declared no potential conflicts of interest with respect to the research, authorship, and/or publication of this article.

Funding

The author(s) disclosed receipt of the following financial support for the research, authorship, and/or publication of this article. This work was supported by the William Demant Foundation and the Swiss National Science Foundation (partial salary of C.A.N).

Author Contributions

C.A.N., D.M.L, J.M., and T.R.B. designed the experiments; C.A.N. performed all experiments and analysis; C.A.N wrote the manuscript; D.M.L, J.M., and T.R.B provided feedback and reviewed the manuscript.

ORCID iDs

Charlotte Amalie Navntoft https://orcid.org/0000-0003-0024-6142

Jeremy Marozeau https://orcid.org/0000-0002-4505-135X

References

Adamson, C. L., Reid, M. A., Mo, Z. L., Bowne-English, J., & Davis, R. L. (2002). Firing features and potassium channel content of murine spiral ganglion neurons vary with cochlear location. *Journal of Comparative Neurology*, *447*(4), 331–350. https://doi.org/10.1002/cne.10244

Advanced Bionics. (2010). SoundWave ™2.0 fitting manual. *Advanced Bionics LLC, CA, US*.

Ballestero, J., Recugnat, M., Laudanski, J., Smith, K. E., Jagger, D. J., Gnansia, D., & McAlpine, D. (2015). Reducing current spread by use of a novel pulse shape for electrical stimulation of the auditory nerve. *Trends in Hearing*, *19*, 233121651561976. https://doi.org/10.1177/2331216515619763

Bates, D., Mächler, M., Bolker, B., & Walker, S. (2015). Fitting linear mixed-effects models using lme4. *Journal of Statistical Software*, *67*(1), 1–48. https://doi.org/10.18637/jss.v067.i01

Beitel, R. E., Vollmer, M., Snyder, R. L., Schreiner, C. E., & Leake, P. A. (2000). Behavioral and neurophysiological thresholds for electrical cochlear stimulation in the deaf cat. *Audiology and Neuro-Otology*, *5*(1), 31–38. https://doi.org/10.1159/000013863

Bierer, J. A., & Litvak, L. (2016). Reducing channel interaction through cochlear implant programming may improve speech perception. *Trends in Hearing*, *20*, 1–12. https://doi.org/10.1177/2331216516653389

Bierer, J. A. (2007). Threshold and channel interaction in cochlear implant users: Evaluation of the tripolar electrode configuration. *The Journal of the Acoustical Society of America*, *121*(3), 1642–1653. https://doi.org/10.1121/1.2436712

Bierer, J. A., & Faulkner, K. F. (2010). Identifying cochlear implant channels with poor electrode-neuron interface: partial tripolar, single-channel thresholds and psychophysical tuning curves. *Ear & Hearing*, *31*(2), 247–258. https://doi.org/10.1097/AUD.0b013e3181c7daf4

Bierer, J. A., & Nye, A. D. (2014). Comparisons between detection threshold and loudness perception for individual cochlear implant channels. *Ear and Hearing*, *35*(6), 641–651. http://journals.lww.com/00003446-201411000-00007

Bonnet, R. M., Frijns, J. H. M., Peeters, S., & Briaire, J. J. (2004). Speech recognition with a cochlear implant using triphasic charge-balanced pulses. *Acta Oto-Laryngologica*, *124*(4), 371–375. https://doi.org/10.1080/00016480410031084

Boulet, J., White, M., & Bruce, I. C. (2016). Temporal Considerations for Stimulating Spiral Ganglion Neurons with Cochlear Implants. *Journal of the Association for Research in Otolaryngology*, *17*(1), 1–17. https://doi.org/10.1007/s10162-015-0545-5

Bruce, I. C., Green, L., V-ghaffari, B., & & Rutherford, M. A. (2019). Poster: Simulating the Effects of "M-current" Potassium Channels in Cochlear Implant Excitation of Auditory Nerve Fibers. *Conference on Implantable Auditory Prostheses (CIAP), July 2019, CA, US*.

Brummer, S. B., & Turner, M. J. (1977). Electrochemical Considerations for Safe Electrical Stimulation of the Nervous System with Platinum Electrodes. *IEEE Transactions on Biomedical Engineering*. *BME*, *24*(1), 59–63. https://doi.org/10.1109/TBME.1977.326218

Carlyon, R. P., van Wieringen, A., Deeks, J. M., Long, C. J., Lyzenga, J., & Wouters, J. (2005). Effect of inter-phase gap on the sensitivity of cochlear implant users to electrical stimulation. *Hearing Research*, *205*(1–2), 210–224. https://doi.org/10.1016/j.heares.2005.03.021

Carney, L. H., & McDonough, J. M. (2019). Nonlinear auditory models yield new insights into representations of vowels. *Attention, Perception, & Psychophysics*, *81*(4), 1034–1046. https://doi.org/10.3758/s13414-018-01644-w

Dai, H., & Micheyl, C. (2010). On the choice of adequate randomization ranges for limiting the use of unwanted cues in same-different, dual-pair, and oddity tasks. *Attention, Perception, & Psychophysics*, *72*(2), 538–547. https://doi.org/10.3758/APP.72.2.538

Dobie, R. A., & Dillier, N. (1985). Some aspects of temporal coding for single-channel electrical stimulation of the cochlea. *Hearing Research*, *18*(1), 41–55. https://doi.org/10.1016/0378-5955(85)90109-1

Ferragamo, M. J., & Oertel, D. (2002). Octopus Cells of the Mammalian Ventral Cochlear Nucleus Sense the Rate of Depolarization. *Journal of Neurophysiology*, *87*(5), 2262–2270. https://doi.org/10.1152/jn.00587.2001

Fraser, M., & McKay, C. M. (2012). Temporal modulation transfer functions in cochlear implantees using a method that limits overall loudness cues. *Hearing Research*, *283*(1–2), 59–69. https://doi.org/10.1016/j.heares.2011.11.009

Gai, Y., Doiron, B., Kotak, V., & Rinzel, J. (2009). Noise-Gated Encoding of Slow Inputs by Auditory Brain Stem Neurons With a Low-Threshold K + Current. *Journal of Neurophysiology*, *102*(6), 3447–3460. https://doi.org/10.1152/jn.00538.2009

Gai, Y., Doiron, B., & Rinzel, J. (2010). Slope-Based Stochastic Resonance: How Noise Enables Phasic Neurons to Encode Slow Signals. *PLoS Computational Biology*, *6*(6), e1000825. https://doi.org/10.1371/journal.pcbi.1000825

Goehring, T., Archer-Boyd, A., Deeks, J. M., Arenberg, J. G., & Carlyon, R. P. (2019). A Site-Selection Strategy Based on Polarity Sensitivity for Cochlear Implants: Effects on Spectro-Temporal Resolution and Speech Perception. *Journal of the Association for Research in Otolaryngology*, *20*(4), 431–448. https://doi.org/10.1007/s10162-019-00724-4

Guérit, F., Marozeau, J., Deeks, J. M., Epp, B., & Carlyon, R. P. (2018). Effects of the relative timing of opposite-polarity pulses on loudness for cochlear implant listeners. *The Journal of the Acoustical Society of America*, *144*(5), 2751–2763. https://doi.org/10.1121/1.5070150

Guérit, F., Marozeau, J., Epp, B., & Carlyon, R. P. (2020). Effect of the Relative Timing between Same-Polarity Pulses on Thresholds and Loudness in Cochlear Implant Users. *Journal of the Association for Research in Otolaryngology*, *21*(6), 497–510. https://doi.org/10.1007/s10162-020-00767-y

Hardie, N. A., & Shepherd, R. K. (1999). Sensorineural hearing loss during development: morphological and physiological response of the cochlea and auditory brainstem. *Hearing Research*, *128*(1–2), 147–165. https://doi.org/10.1016/S0378-5955(98)00209-3

Hughes, M. L., & Stille, L. J. (2009). Psychophysical and physiological measures of electrical-field interaction in cochlear implants. *The Journal of the Acoustical Society of America*, *125*(1), 247–260. https://doi.org/10.1121/1.3035842

Imennov, N. S., & Rubinstein, J. T. (2009). Stochastic Population Model for Electrical Stimulation of the Auditory Nerve. *IEEE Transactions on Biomedical Engineering*, *56*(10), 2493–2501. https://doi.org/10.1109/TBME.2009.2016667

Izhikevich, E. M. (2007). *Dynamical Systems in Neuroscience: The Geometry of Excitability and Bursting*. (T. J. Sejnowski & T. A. Poggio (eds.). The MIT Press.

Jesteadt, W. (1980). An adaptive procedure for subjective judgments. *Perception & Psychophysics*, *28*(1), 85–88. https://doi.org/10.3758/BF03204321

Johnston, J., Forsythe, I. D., & Kopp-Scheinpflug, C. (2010). Going native: Voltage-gated potassium channels controlling neuronal

excitability. *Journal of Physiology*, *588*(17), 3187–3200. https://doi.org/10.1113/jphysiol.2010.191973

Joshi, S., Dau, T., & Epp, B. (2017). A Model of Electrically Stimulated Auditory Nerve Fiber Responses with Peripheral and Central Sites of Spike Generation. *JARO - Journal of the Association for Research in Otolaryngology*, *18*(2), 323–342. https://doi.org/10.1007/s10162-016-0608-2

Joshi, S., Marozeau, J., & Epp, B. (2017). Poster: Low-threshold potassium channels and their effect on polarity sensitivity of the electrically stimulated auditory nerve. *Conference on Implantable Auditory Prostheses (CIAP), July 2017, CA, US*.

Kawase, T., & Liberman, M. (1992). Spatial organization of the auditory nerve according to spontaneous discharge rate. *The Journal of Comparative Neurology*, *319*(2), 312–318. https://pubmed.ncbi.nlm.nih.gov/1381729/.

Kreft, H. A., Donaldson, G. S., & Nelson, D. A. (2004). Effects of pulse rate on threshold and dynamic range in Clarion cochlear-implant users (L). *The Journal of the Acoustical Society of America*, *115*(5), 1885–1888. https://doi.org/10.1121/1.1701895

Kuznetsova, A., Brockhoff, P. B., & Christensen, R. H. B. (2017). lmerTest Package: Tests in Linear Mixed Effects Models. *Journal of Statistical Software*, *82*(13), 1–26. https://doi.org/10.18637/jss.v082.i13

Kuznetsova, A., Christensen, R. H. B., Bavay, C., & Brockhoff, P. B. (2015). Automated mixed ANOVA modeling of sensory and consumer data. *Food Quality and Preference*, *40*(PA), 31–38. https://doi.org/10.1016/j.foodqual.2014.08.004

Landsberger, D. M., Padilla, M., & Srinivasan, A. G. (2012). Reducing current spread using current focusing in cochlear implant users. *Hearing Research*, *284*(1–2), 16–24. http://dx.doi.org/10.1016/j.heares.2011.12.009

Landsberger, D. M., Svrakic, M., Roland, J. T., & Svirsky, M. (2015). The Relationship Between Insertion Angles, Default Frequency Allocations, and Spiral Ganglion Place Pitch in Cochlear Implants. *Ear and Hearing*, *36*(5), e207–e213. http://journals.lww.com/00003446-201509000-00015

Landsberger, D. M., Vermeire, K., Claes, A., Van Rompaey, V., & Van de Heyning, P. (2016). Qualities of Single Electrode Stimulation as a Function of Rate and Place of Stimulation with a Cochlear Implant. *Ear & Hearing*, *37*(3), e149–e159. https://doi.org/10.1097/AUD.0000000000000250

Leake, P., Snyder, R., & Hradek, G. (1993). Spatial organization of inner hair cell synapses and cochlear spiral ganglion neurons. *The Journal of Comparative Neurology*, *333*(2), 257–270. https://pubmed.ncbi.nlm.nih.gov/8345106/

Lenth, R., Singmann, H., Love, J., Buerkner, P., & Herve, M. (2021). emmeans-package: Estimated Marginal Means, aka Least-Squares Means. Version 1.7.0. *IA, US*. https://github.com/rvlenth/emmeans

Levitt, H. (1971). Transformed up-down methods in psychoacoustics. *The Journal of the Acoustical Society of America*, *49*(2), 467–477. http://www.ncbi.nlm.nih.gov/pubmed/5541744

Liberman, M. (1980). Morphological differences among radial afferent fibers in the cat cochlea: An electron-microscopic study of serial sections. *Hearing Research*, *3*(1), 45–63. https://doi.org/10.1016/0378-5955(80)90007-6

Liberman, M. (1982). The cochlear frequency map for the cat: labeling auditory-nerve fibers of known characteristic frequency. *The Journal of the Acoustical Society of America*, *72*(5), 1441–1449. https://pubmed.ncbi.nlm.nih.gov/7175031/

Liberman, M. C., & Oliver, M. E. (1984). Morphometry of intracellularly labeled neurons of the auditory nerve: Correlations with functional properties. *The Journal of Comparative Neurology*, *223*(2), 163–176. http://doi.wiley.com/10.1002/cne.902230203

Litovsky, R. Y., Goupell, M. J., Kan, A., & Landsberger, D. M. (2017). Use of Research Interfaces for Psychophysical Studies With Cochlear-Implant Users. *Trends in Hearing*, *21*, 233121651773646. https://doi.org/10.1177/2331216517736464

Long, C. J., Holden, T. A., McClelland, G. H., Parkinson, W. S., Shelton, C., Kelsall, D. C., & Smith, Z. M. (2014). Examining the Electro-Neural Interface of Cochlear Implant Users Using Psychophysics, CT Scans, and Speech Understanding. *Journal of the Association for Research in Otolaryngology*, *15*(2), 293–304. https://doi.org/10.1007/s10162-013-0437-5

Macherey, O., Carlyon, R. P., Chatron, J., & Roman, S. (2017). Effect of Pulse Polarity on Thresholds and on Non-monotonic Loudness Growth in Cochlear Implant Users. *Journal of the Association for Research in Otolaryngology*, *18*(3), 513–527. https://doi.org/10.1007/s10162-016-0614-4

Macherey, O., van Wieringen, A., Carlyon, R. P., Deeks, J. M., & Wouters, J. (2006). Asymmetric Pulses in Cochlear Implants: Effects of Pulse Shape, Polarity, and Rate. *Journal of the Association for Research in Otolaryngology*, *7*(3), 253–266. https://doi.org/10.1007/s10162-006-0040-0

Marks, L. E., & Florentine, M. (2011). Measurement of Loudness, Part I: Methods, Problems, and Pitfalls. In Florentine, M., Popper, A. N., & Fay, R. R. (Eds.), (pp. 17–56). Springer. https://doi.org/10.1007/978-1-4419-6712-1_2

Marozeau, J., McDermott, H. J., Swanson, B. A., & McKay, C. M. (2015). Perceptual Interactions Between Electrodes Using Focused and Monopolar Cochlear Stimulation. *Journal of the Association for Research in Otolaryngology*, *16*(3), 401–412. https://doi.org/10.1007/s10162-015-0511-2

McGinley, M. J., & Oertel, D. (2006). Rate thresholds determine the precision of temporal integration in principal cells of the ventral cochlear nucleus. *Hearing Research*, *216–217*(1–2), 52–63. https://doi.org/10.1016/j.heares.2006.02.006

McKay, C. M., & Henshall, K. R. (2003). The perceptual effects of interphase gap duration in cochlear implant stimulation. *Hearing Research*, *181*(1–2), 94–99. https://doi.org/10.1016/S0378-5955(03)00177-1

McKay, C. M., Lim, H. H., & Lenarz, T. (2013). Temporal Processing in the Auditory System. *Journal of the Association for Research in Otolaryngology*, *14*(1), 103–124. https://doi.org/10.1007/s10162-012-0354-z

Merchan-Perez, A., & Liberman, M. (1996). Ultrastructural differences among afferent synapses on cochlear hair cells: correlations with spontaneous discharge rate. *The Journal of Comparative Neurology*, *371*(2), 208–221. https://pubmed.ncbi.nlm.nih.gov/8835727/

Miller, C. A., Abbas, P. J., Robinson, B. K., Rubinstein, J. T., & Matsuoka, A. J. (1999). Electrically evoked single-fiber action potentials from cat: Responses to monopolar, monophasic stimulation. *Hearing Research*, *130*(1–2), 197–218. https://doi.org/10.1016/S0378-5955(99)00012-X

Mo, Z. L., Adamson, C. L., & Davis, R. L. (2002). Dendrotoxin-sensitive K+ currents contribute to accomodation in murine spiral ganglion neurons. *Journal of Physiology*, *542*(3), 763–778. https://doi.org/10.1113/jphysiol.2002.017202

Nadol, J. (1997). Patterns of neural degeneration in the human cochlea and auditory nerve: Implications for cochlear implantation. *Otolaryngology - Head and Neck Surgery*, *117*(3 I), 220–228. https://doi.org/10.1016/s0194-5998(97)70178-5

Navntoft, C. A., Marozeau, J., & Barkat, T. R. (2020). Ramped pulse shapes are more efficient for cochlear implant stimulation in an animal model. *Scientific Reports*, *10*(1), 3288. https://doi.org/10.1038/s41598-020-60181-5

Negm, M. H., & Bruce, I. C. (2014). The Effects of HCN and KLT Ion Channels on Adaptation and Refractoriness in a Stochastic Auditory Nerve Model. *IEEE Transactions on Biomedical Engineering*, *61*(11), 2749–2759. https://doi.org/10.1109/TBME.2014.2327055

Parkins, C. W., & Colombo, J. (1987). Auditory-nerve single-neuron thresholds to electrical stimulation from scala tympani electrodes. *Hearing Research*, *31*(3), 267–285. https://doi.org/10.1016/0378-5955(87)90196-1

Peeters, G., Giordano, B. L., Susini, P., Misdariis, N., & McAdams, S. (2011). The Timbre Toolbox: Extracting audio descriptors from musical signals. *The Journal of the Acoustical Society of America*, *130*(5), 2902–2916. https://doi.org/10.1121/1.3642604

R Core Team. (2015). *R: A language and environment for statistical computing*. R Foundation for Statistical Computing.

Rutherford, M. A., Chapochnikov, N. M., & Moser, T. (2012). Spike encoding of neurotransmitter release timing by spiral ganglion neurons of the cochlea. *Journal of Neuroscience*, *32*(14), 4773–4789. https://doi.org/10.1523/JNEUROSCI.4511-11.2012

Schwarz, J. R., Reid, G., & Bostock, H. (1995). Action potentials and membrane currents in the human node of Ranvier. *Pflugers Archiv European Journal of Physiology*, *430*(2), 283–292. https://doi.org/10.1007/BF00374660

Searle, S. R., Speed, F. M., & Milliken, G. A. (1980). Population Marginal Means in the Linear Model: An Alternative to Least Squares Means. *The American Statistician*, *34*(4), 216. https://doi.org/10.2307/2684063

Shannon, R. V. (1992). A model of safe levels for electrical stimulation. *IEEE Transactions on Biomedical Engineering*, *39*(4), 424–426. https://doi.org/10.1109/10.126616

Shannon, R. V. (1985). Threshold and loudness functions for pulsatile stimulation of cochlear implants. *Hearing Research*, *18*(2), 135–143. https://doi.org/10.1016/0378-5955(85)90005-X

Shannon, R. V. (1989). A model of threshold for pulsatile electrical stimulation of cochlear implants. *Hearing Research*, *40*(3), 197–204. https://doi.org/10.1016/0378-5955(89)90160-3

Shepherd, R. K., & Javel, E. (1999). Electrical stimulation of the auditory nerve: II. Effect of stimulus waveshape on single fibre response properties. *Hearing Research*, *130*(1–2), 171–188. https://doi.org/10.1016/S0378-5955(99)00011-8

Skinner, M. W., Holden, L. K., Holden, T. A., & Demorest, M. E. (2000). Effect of stimulation rate on cochlear implant recipients' thresholds and maximum acceptable loudness levels. *Journal of the American Academy of Audiology*, *11*(4), 203–213.

Skinner, M. W., Ketten, D. R., Holden, L. K., Harding, G. W., Smith, P. G., Gates, G. A., Neely, J. G., Kletzker, G. R., Brunsden, B., & Blocker, B. (2002). CT-Derived Estimation of Cochlear Morphology and Electrode Array Position in Relation to Word Recognition in Nucleus-22 Recipients. *Journal of the Association for Research in Otolaryngology*, *3*(3), 332–350. https://doi.org/10.1007/s101620020013

Smith, K. E., Browne, L., Selwood, D. L., McAlpine, D., & Jagger, D. J. (2015). Phosphoinositide modulation of heteromeric Kv1 channels adjusts output of spiral ganglion neurons from hearing mice. *Journal of Neuroscience*, *35*(32), 11221–11232. https://doi.org/10.1523/JNEUROSCI.0496-15.2015

Svirskis, G., Kotak, V., Sanes, D. H., & Rinzel, J. (2002). Enhancement of Signal-to-Noise Ratio and Phase Locking for Small Inputs by a Low-Threshold Outward Current in Auditory Neurons. *The Journal of Neuroscience*, *22*(24), 11019–11025. https://doi.org/10.1523/JNEUROSCI.22-24-11019.2002

Undurraga, J. A., Carlyon, R. P., Macherey, O., Wouters, J., & van Wieringen, A. (2012). Spread of excitation varies for different electrical pulse shapes and stimulation modes in cochlear implants. *Hearing Research*, *290*(1–2), 21–36. https://doi.org/10.1016/j.heares.2012.05.003

Vallbo, A., & Johansson, R. (1976). Skin mechanoreceptors in the human hand: Neural and psychophysical thresholds. In Zotterman, Y. (Ed.), *Sensory Functions of the Skin in Primates* (pp. 185–197). Pergamon Press.

Van Wieringen, A., Carlyon, R. P., Laneau, J., & Wouters, J. (2005). Effects of waveform shape on human sensitivity to electrical stimulation of the inner ear. *Hearing Research*, *200*(1–2), 73–86. https://doi.org/10.1016/j.heares.2004.08.006

Vandali, A. E., Whitford, L. A., Plant, K. L., & Clark, G. M. (2000). Speech perception as a function of electrical stimulation rate: Using the nucleus 24 cochlear implant system. *Ear and Hearing*, *21*(6), 608–624. https://doi.org/10.1097/00003446-200012000-00008

Vanpoucke, F. J., Zarowski, A. J., & Peeters, S. A. (2004). Identification of the impedance model of an implanted cochlear prosthesis from intracochlear potential measurements. *IEEE Transactions on Biomedical Engineering*, *51*(12), 2174–2183. https://doi.org/10.1109/TBME.2004.836518

Yip, M., Bowers, P., Noel, V., Chandrakasan, A., & Stankovic, K. M. (2017). Energy-efficient waveform for electrical stimulation of the cochlear nerve. *Scientific Reports*, *7*(1), 1–9. https://doi.org/10.1038/s41598-017-13671-y